Thermodynamic properties of (Gd,Pr)$OsGa_4$ Intermetallic Compounds

B. Sondezi[1], **R Djoumessi Fobasso**[1]

[1]Rare Earth-Based oxides and Nano Group, Department of Physics, University of Johannesburg, Auckland Park 2006, South Africa

E-mail: `redrissed@uj.ac.za`

Abstract. Intermetallic compounds containing rare-earth and transition metals exhibit rich magnetic and electronic properties, making them crucial for understanding correlated electron systems. Among these, the layered compounds $PrOsGa_4$ and $GdOsGa_4$ are particularly intriguing due to their interplay of localized 4f moments and conduction electrons, prompting a detailed investigation of their physical behavior. For this purpose, polycrystalline samples of $PrOsGa_4$ and $GdOsGa_4$ were prepared by arc-melting technique using high-purity elemental constituent elements. The Rietveld crystal structure refinement of powder X-ray diffraction patterns with a full-profile refinement confirms that both samples crystallize in the orthorhombic $CeOsGa_4$-structure type with space group Pmma (number 51). The structure exhibits two types of two dimensionally alternating layers that are slightly puckered, having $OsGa_3$ layer sandwiched between Pr(Gd)Ga layers. Here, we present the physical properties of these compounds through temperature (T) dependent magnetic susceptibility $\chi(T)$ and magnetization $M(B)$, heat capacity $C_\mathrm{p}(T)$, and electrical resistivity $\rho(T)$. They consistently reveal that the compounds undergo an antiferromagnetic/ferromagnetic type orderings below 14 K and 16 K for $GdOsGa_4$ and $PrOsGa_4$, respectively. The $\chi(T)$ data obey the Curie-Weiss law above 50 K. The layered structure and tunable electronic properties of these materials could inspire further exploration where control of 4f-electron interactions with conduction electrons is critical. The study may therefore contribute towards a better understanding of the physics of this class of materials.

1 Introduction

Gallium (Ga)-rich intermetallic compounds have recently drawn significant attention due to their structural complexity and tunable electronic/magnetic properties, which are relevant for advanced technologies such as cryogenic cooling [1]. Amongst the first reported Ga-rich compounds, there are $\mathrm{RE_2Co_3Ga_9}$ (RE: Y, Ho) [2, 3], and $\mathrm{RE_2T_3Ge_9}$ (RE: Y, Sm, Gd-Yb; T: Rh, Ir) [4]. In these series, there is a layered arrangement of the T-Ga atoms and the RE ions reside in interstitial sites. Moreover, the rare-earth ions dominate the magnetism in these materials with paramagnetism at high temperatures and either antiferromagnetic (AFM) or ferromagnetic (FM) orderings at low temperatures depending on the rare-earth of interest. It also depends on the transition element. For instance, in Co-based compounds in this series, the rare-earth ions dominate the magnetic behavior since the Co atoms are non magnetic or exhibit a weak magnetism. However, others such as Fe- or Ru- based may exhibit stronger magnetic interactions. Gd^{3+} ions often leads to strong magnetic ordering while Pr^{3+} ions usually exhibits crystalline electric field effects. This can lead to interesting properties. Despite their potential, Gd- and Pr-based variants in this family remain understudied. We therefore report on the physical properties of $PrOsGa_4$ and $GdOsGa_4$ compounds. This will give us an insight into the low-temperature magnetic transitions in these materials and serves as model systems for studying 4f-electron correlations in layered materials.

2 Synthesis and experimental details

Stoichiometric quantities of the elements Pr, Gd, Os, Ga were accurately weighed and arc-melted under ultra high purity argon atmosphere, on a water cooled copper hearth. The samples were remelted three times, to promote homogeneity. The final as-cast ingot was then wrapped in tantalum foil, sealed under vacuum in an evacuated quartz tube and annealed at 1200° C for 14 days to improve the homogeneity and followed by quenching into cold water. The phase purity of the annealed sample was checked by performing powder X-ray diffraction (XRD) experiments at room temperature using Cu-kα radiation of wavelength 1.54 Å on a Rigaku powder diffractometer. The obtained XRD spectra were analyzed by Rietveld refinement method using the FULLPROF software. The magnetic properties were performed by a commercial Quantum Design Dynacool system, in the temperature range, 2 K - 380 K and applied magnetic field up to 9 T. The specific heat $C_\mathrm{P}(T)$ measurement was carried out in the same Dynacool system using a thermal relaxation method in temperature range of 2 K–300 K. The temperature dependent resistivity $\rho(T)$ were measured by the standard four–probe ac–method using the same apparatus.

3 Results and Discussion

3.1 Structural properties

The Rietveld crystal structure refinement of the room-temperature powder XRD patterns of both samples are displayed in Figure 1. The samples form in the orthorhombic $\mathrm{CeOsGa_4}$ structure type (space group Pmma, number 51). The obtained lattice parameters are reported in the table 1 below. The structure exhibits two types of two dimensionally alternating layers that are slightly puckered, having $\mathrm{OsGa_3}$ layer sandwiched between Pr(Gd)Ga layers and is presented in figure 2.

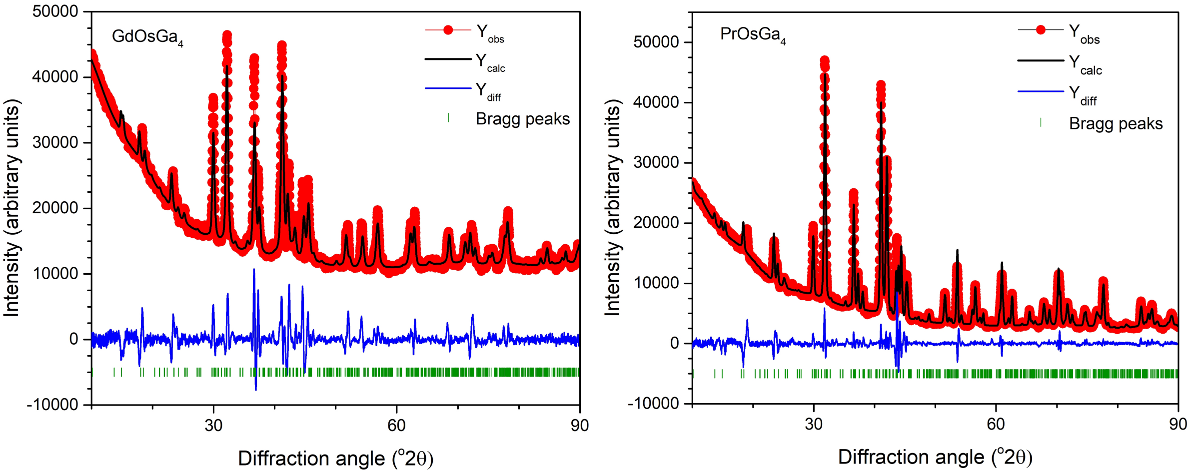

Figure 1: Powder X-ray diffraction of both compounds. The red symbols represent the experimental data and the black line represents the calculated data. The difference between experimental and calculated data is shown as a blue line. A set of vertical green bars represent the Bragg peak positions of the $\mathrm{CeOsGa_4}$ structure.

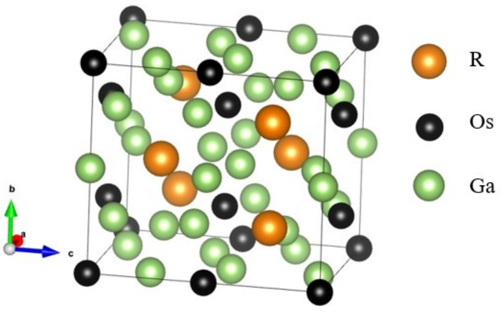

Figure 2: Crystal structure of $\mathrm{ROsGa_4}(\mathrm{R} = \mathrm{Pr}, \mathrm{Gd})$

Table 1: The lattice parameters of $PrOsGa_4$ and $GdOsGa_4$.

Compound	a (Å)	b (Å)	c (Å)	V $(Å)^3$
$PrOsGa_4$	9.59720 (5)	8.90463 (5)	7.744332 (5)	661.83(2)
$GdOsGa_4$	9.487082 (5)	8.954183 (5)	7.699494 (5)	654.065(4)

3.2 Magnetic properties

The temperature dependences of magnetic susceptibility $\chi(T)$ of $GdOsGa_4$ and $PrOsGa_4$ measured in an applied magnetic field B = 0.01 T and in field cooled mode are shown in Figure 3. The high-temperature regions of both compounds (T $\geq$ 50 K) both follow the Curie-Weiss law given by expression 1.

$$\chi(T) = \chi_0 + C/(T - \theta_{\mathrm{P}}), \tag{1}$$

where χ_0 is the temperature independent susceptibility, C is the Curie-Weiss constant, and θ_{P} is the paramagnetic Weiss temperature. From the least-squares fit of equation (1) to the $GdOsGa_4$ data, we obtained an effective magnetic moment μ_{eff} = 8.191 (3) μ_{B}/Gd^{3+} ion and a Weiss temperature θ_{P} = -21.791 (3) K. The negative value of the paramagnetic Weiss temperature indicates the dominance of antiferromagnetic interactions in the high temperature region of $GdOsGa_4$. The μ_{eff} value informs that Gd ions are fully responsible for the magnetism in this material as the obtained value is very close and in agreement with the theoretical value of Gd^{3+} ions, which is 7.94 μ_{B}. Similarly, the least-squares fit of equation (1) to the $PrOsGa_4$ data leads to a calculated effective magnetic moment μ_{eff} of 3.67 (2) μ_{B}/Pr^{3+} ion and a negative paramagnetic Weiss temperature θ_{P} = -1.19 (1) K. The obtained negative θ_{P} value confirms the antiferromagnetic coupling of the Pr^{3+} ions in this system, whilst the effective magnetic moment value is close to the theoretical value of 3.58 μ_{B}/Pr^{3+} ions.

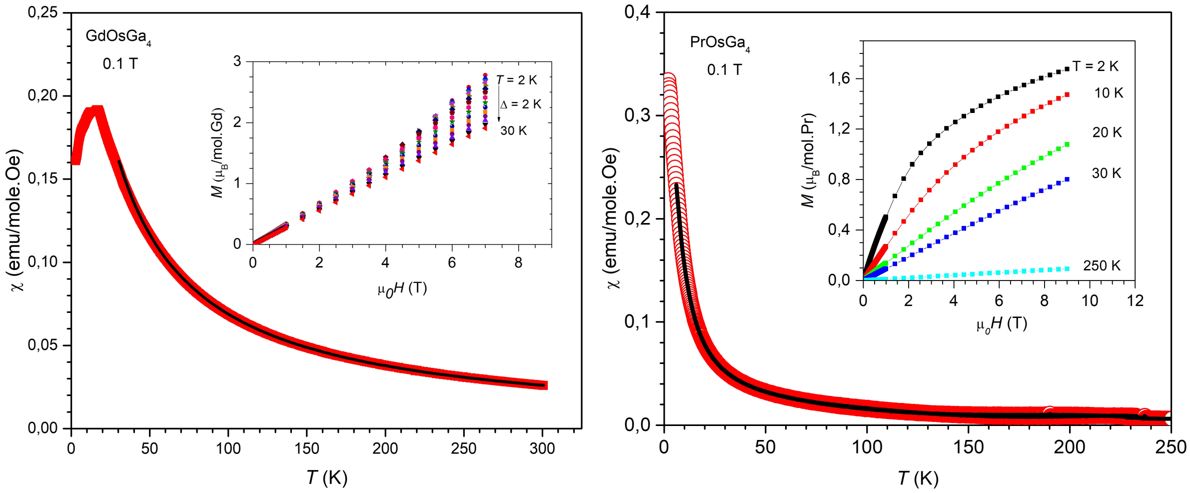

Figure 3: Main panel: The red curve represents the temperature dependence of dc-magnetic susceptibility under an applied field value of 0.1 T for $GdOsGa_4$. The black line represents the Curie-Weiss fit as explained in the text. Inset: magnetization isotherms below and above the transition temperature.

A kink deviation from linearity is observed at T_{N} = 14 K for $GdOsGa_4$ and marks an onset of an antiferromagnetic ground state ordering. This is due to an emergence of an antiparallel ordering which reduces the magnetic response of the system compared to the paramagnetic phase. Similary, at T_{C} = 16 K, a deviation from linearity is observed in $PrOsGa_4$ and it is associated this time to a ferromagnetic ordering which arises from spontaneous magnetization.

The inset of the left panel of Figure 3(a) shows the magnetization data of $GdOsGa_4$ measured from 2 K to 30 K with intervals of 2 K. These includes temperatures below and above the transition temperature. All measured isotherms show linear behaviour over the entire applied magnetic field range, confirming long range antiferromagnetic ordering even for data measured well below the ordering temperature. This observation is consistent with the antiferromagnetic ordering observed in the $\chi(T)$ data and can be the sign of weakly interacting local moments when the exchange coupling is negligible compared to the Zeeman energy. Similarly, the magnetization data of PrOsGa$_4$ were measured but in 2, 10, 20 and 30 K. The data at 2 K and 10 K shows a slight curvature at low applied magnetic fields but does not fully saturate up to 9.0 T. This confirms the presence of short-range correlation in the paramagnetic region.

3.3 Specific heat

The temperature dependences of specific heat of GdOsGa$_4$ and PrOsGa$_4$ are shown in figure 4. The data were measured from room temperature down to 1.8 K in zero applied magnetic field. The high temperature data upto T= 280 K reaches the Dulong Petit approximation (green line in figure 4), giving a value of 142 J/mol.K, which is in close agreement with the theoretical value of 149 J/mol.K, as calculated from 3NR (where N is the number of atoms per formula unit and R is the universal gas constant). A similar behavior has been observed in PrOsGa$_4$ and is commonly observed in normal metals. The kink observed around the transition temperatures, T_{c}= 14 K for GdOsGa$_4$ and T_{c}= 16 K for PrOsGa$_4$ is a sign of a short-range order-like transition. This corroborates with the results obtained with $\chi(T)$.

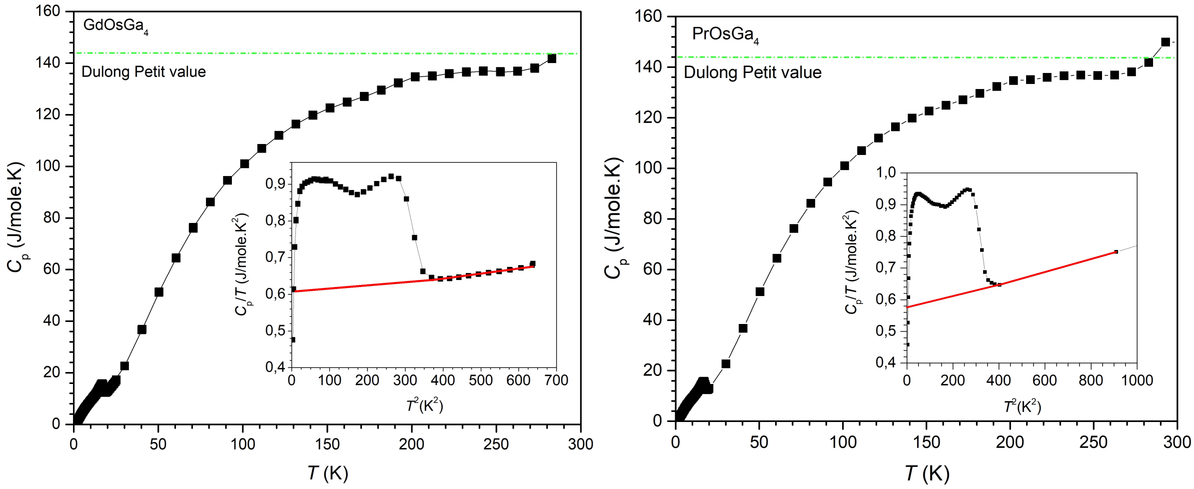

Figure 4: Temperature variations of specific heat capacity of GdOsGa$_4$ (left panel) and PrOsGa$_4$ (right panel), measured in zero field from 300 K to 1.8 K. The insets in both graphs represent the plot of $C_{\mathrm{P}}(T)/T$ vs T^2 for both compounds. The red line represents the linear fit used to estimate the Sommerfeld coefficient as explained in the text.

The insets of figure 4 shows the C_{P}/T vs T^2 curves, with the Debye fit of the data just above the ordering temperature in both cases, represented by a red line. The red line is the fit according to the expression:

$$\frac{C_{\mathrm{P}}}{T} = \gamma + \beta T^2, \tag{2}$$

where γ is the Sommerfeld coefficient and β is the constant associated with the Debye temperature θ_{D}. The first term is the electronic contribution and the second term is the lattice (phononic) contribution.

The Sommerfeld coefficient is found to be $\gamma = 0.5876(2)$ J/mol.K^2, and $\gamma = 0.5645(1)$ J/mol.K^2 for GdOsGa$_4$, and PrOsGa$_4$, respectively. These value suggests that the compounds belong to the heavy-fermion family.

4 Electrical resistivity

The electrical resistivity, $\rho(T)$, of GdOsGa$_4$ and PrOsGa$_4$, measured in zero applied magnetic field and from 300 K to 2 K are displayed in figure 5. It decreases with decreasing temperature, which indicates the metallic nature of the compound GdOsGa$_4$. Similar metallic behavior has also been observed for PrOsGa$_4$. Towards high temperatures, the Bloch-Grüneisen function predicts a linear-in-T behavior of the electrical resistivity for both compounds. A curvature on the other hand is attributable to intraband scattering when for example there is a semi-filled d-electron

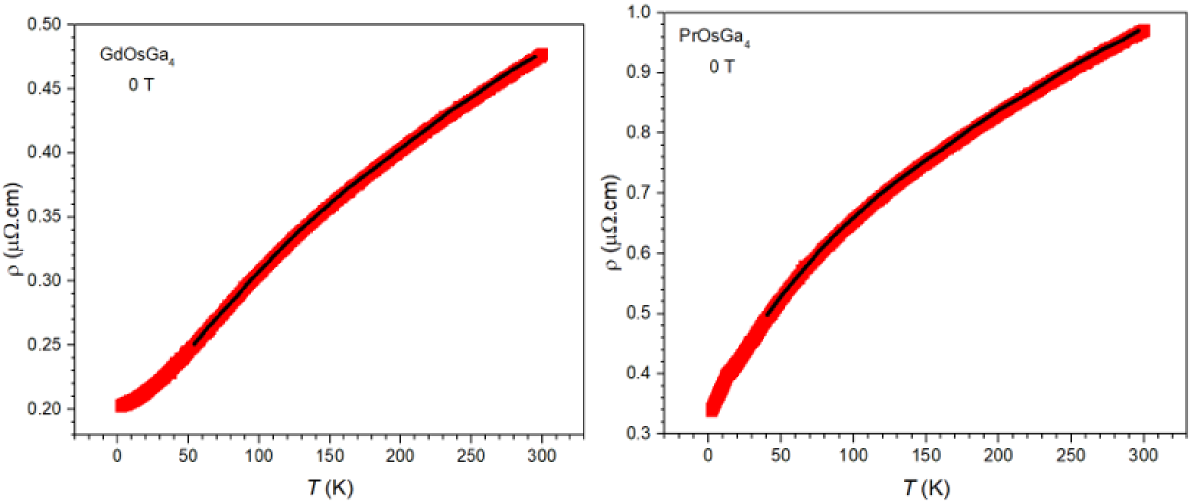

Figure 5: Temperature dependence of electrical resistivity of GdOsGa$_4$ and PrOsGa$_4$ measured in zero applield magnetic field. The black lines represent the Bloch-Grüneisen fit as explained in the text.

band. In order to establish the electron-phonon correlation, the experimental data of GdOsGa$_4$ and PrOsGa$_4$ were fitted by the Bloch-Grüneisen relationship given by Eq 3 below.

$$\rho(T) = \rho_0 + \frac{4A_0}{\theta_\mathrm{R}}\left(\frac{T}{\theta_\mathrm{R}}\right)^5 \int_0^{\theta_\mathrm{R}/T} \frac{x^5 dx}{(e^x - 1)(1 - e^x)} \tag{3}$$

where ρ_0 is the residual resistivity due to impurities and imperfections in the crystal lattice. A_0 is the electron-phonon coupling constant and θ_R is a characteristic energy scale of lattice vibrations sometimes referred to as the resistivity Debye temperature. The best least-squares fit of Eq. 3 to the experimental $\rho(T)$ data of both compounds yielded the parameters given in the table below.

Table 2: Parameters derived from the Bloch-Grüneisen fit of PrOsGa$_4$ and GdOsGa$_4$.

Compound	ρ_0 ($\mu\Omega$.cm)	A$_0$ ($\mu\Omega$.cm.K^{-8})	θ_R (K)
GdOsGa$_4$	0.217(2)	5.90(2)	259.4(2)
PrOsGa$_4$	0.521(2)	9.92(1)	200.5(2)

5 Conclusion

The study provided a comprehensive study of the structural, magnetic and physical properties of the two intermetallic compounds GdOsGa$_4$ and PrOsGa$_4$. Both compounds, GdOsGa$_4$ and PrOsGa$_4$ crystallize in the same orthorhombic CeOsGa$_4$-type structure belonging to the Pmma space group. A magnetic behavior is observed in both materials. GdOsGa$_4$ data exhibit clear antiferromagnetic ordering at T_N = 14 K while PrOsGa$_4$ is ferromagnetic at T_C = 16 K. These results are corroborated by magnetic susceptibility, magnetization, and specific heat measurements, which also confirm the dominance of localized 4f moments in both systems. Electrical resistivity measurements further affirm the metallic nature of both compounds, with electron-phonon interactions well-described by the Bloch-Grüneisen model. In summary, this work elucidates the interplay between localized 4f moments and conduction electrons in layered intermetallics, providing a foundation for future studies on tunable magnetic and electronic properties in rare-earth-based materials.

References

[1] N. Shohata, "Magnetic properties of rare earth gallium intermetallic compounds," *Journal of the Physical Society of Japan*, vol. 42, no. 6, pp. 1873–1880, 1977.

[2] J. Niermann, B. Fehrmann, M. W. Wolff, and W. Jeitschko, “Preparation and crystal structure of ternary rare-earth platinum metal aluminides $\mathrm{R_2T_3Al_9}$ (T= Rh, Ir, Pd) with $\mathrm{Y_2Co_3Ga_9}$-type structure and magnetic properties of the iridium compounds,” *Journal of Solid State Chemistry*, vol. 177, no. 7, pp. 2600–2609, 2004.

[3] C. Routsi and J. Yakinthos, “Crystal structure and magnetic properties of $\mathrm{R_2Co_3Al_9}$ compounds (R= Y, Pr, Gd, Tb, Dy, Ho, Er, Tm),” *Journal of alloys and compounds*, vol. 323, pp. 427–430, 2001.

[4] O. Sichevych, W. Schnelle, Y. Prots, U. Burkhardt, and Y. Grin, “Crystal structure and physical properties of new ternary gallides $\mathrm{Eu_2Rh_3Ga_9}$ and $\mathrm{Eu_2Ir_3Ga_9}$,” *Zeitschrift für Naturforschung B*, vol. 61, no. 7, pp. 904–911, 2006.